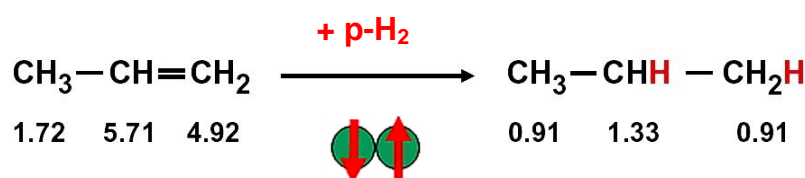


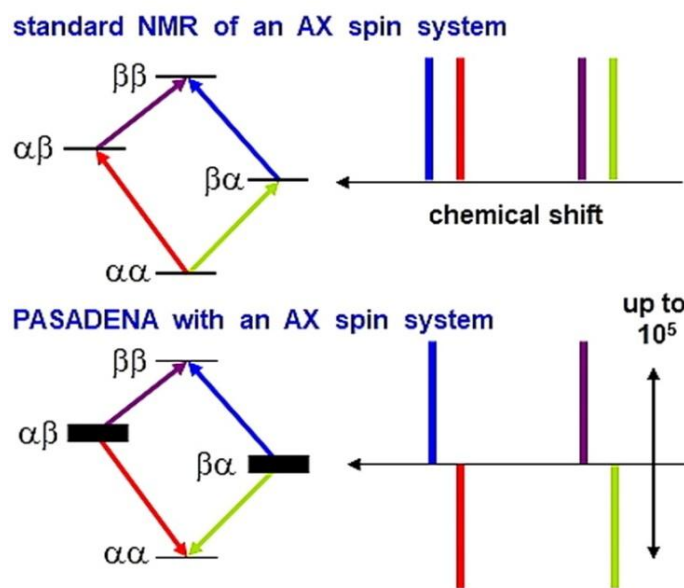
## ***In situ* solid-state NMR studies of parahydrogen-induced polarization on noble metal-loaded catalysts under continuous flow conditions**

**Spectroscopic background:** In contrast to orthohydrogen with the total nuclear spin  $I = 1$ , parahydrogen ( $p\text{-H}_2$ ) has no total nuclear spin (**Fig. 1, middle**) and, therefore, it does not cause a  $^1\text{H}$  NMR signal. By the **pairwise incorporation of the two H atoms of a  $p\text{-H}_2$  molecule into another molecule**, such as propene (see **Fig. 1** with  $^1\text{H}$  chemical shifts at bottom) the symmetry of the parahydrogen is broken and the initial spin order is converted into a **large non-equilibrium spin polarization, called hyperpolarization** ( $\alpha\beta$  and  $\beta\alpha$  in **Scheme 1**) [1-3].



**Fig. 1**

**Parahydrogen-induced polarization (PHIP)** can lead to **enhancements of NMR signal intensities** by more than **three orders of magnitude** [3]. Normal hydrogen ( $n\text{-H}_2$ ) has a para to ortho ratio of 1 to 3, which can be converted to 1 to 1, e.g., by contacting gaseous hydrogen with a conversion catalyst at low temperature, such as iron oxide at  $T = 77\text{ K}$  [3, 4]. There are two different protocols of experiments for NMR studies of PHIP. According to the ALTADENA (adiabatic longitudinal transport after dissociation engenders net alignment) protocol, the hydrogenation reaction with parahydrogen is performed at zero field and, subsequently, the hydrogenated compound is adiabatically transported into a high magnetic field. In this case, multiplets of polarized spins with opposite signs occur in the NMR spectrum [3, 5-7]. The second protocol, called **PASADENA (parahydrogen and synthesis allow dramatically enhanced nuclear alignment)**, is characterized by performing the **hydrogenation reaction with parahydrogen in a high magnetic field**, e.g. the  $B_0$  field of an NMR spectrometer. In this case, antiphase signals are obtained for the hydrogen atoms, which were pairwise incorporated into the reactant molecules. The positive signals in **Scheme 1**, bottom, are due to transitions  $\beta\alpha \rightarrow \beta\beta$  (blue) and  $\alpha\beta \rightarrow \beta\beta$  (violet), while the negative signals are caused by transitions  $\alpha\beta \rightarrow \alpha\alpha$  (red) and  $\beta\alpha \rightarrow \alpha\alpha$  (green) [3, 4, 8].



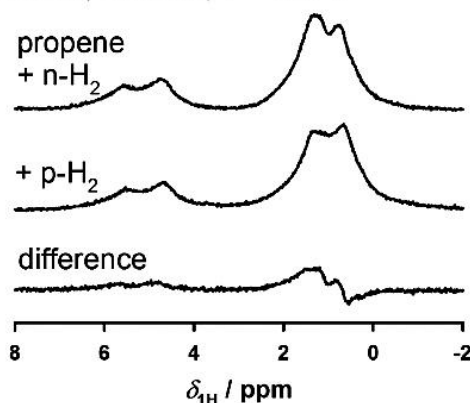
Scheme 1

With the *in situ* flow MAS NMR technique (see Topic 3 of link “*In Situ* Solid-State NMR Techniques”), investigations of the formation of hyperpolarized hydrocarbons, e.g., by the gas phase hydrogenation of propene with parahydrogen at noble metal-loaded support materials acting as catalysts are possible.

Steric limitations of pores in solid catalysts restrict the mobility of the reactant molecules after their adsorption, which causes a broadening of their NMR signals. Since this signal broadening is mainly due to the anisotropy of chemical shielding and dipolar interactions, application of the MAS technique can average most of these interactions. For demonstrating the line-narrowing effect of MAS for NMR signals of hyperpolarized compounds, **Figs. 2a and 2b** show *in situ*  $^1\text{H}$  solid-state NMR spectra recorded during the hydrogenation of propene with  $p\text{-H}_2$  on a silica loaded with 0.9 wt.-% Pt (0.9Pt/silica) at  $T = 298$  K without MAS and with MAS, respectively [9]. The difference spectra shown at the bottom of **Figs. 2a and 2b** indicate that application of MAS causes a significant narrowing of the antiphase signals at 0.8 to 1.6 ppm due to hyperpolarised propane. This observation indicates that the hyperpolarized reaction products of the hydrogenation of propene with  $p\text{-H}_2$  are located on the surface and inside catalyst pores accompanied by significant spin interactions of these product molecules with nuclei in the walls of the host material. Hence, **application of the MAS technique in combination with an *in situ* flow probe is an important prerequisite for the study of PHIP in heterogeneous catalysis** [9-12].

### *In situ* $^1\text{H}$ continuous flow solid-state NMR

a) 0.9Pt/silica, no MAS,  $T = 298\text{ K}$



b) 0.9Pt/silica, MAS,  $T = 298\text{ K}$

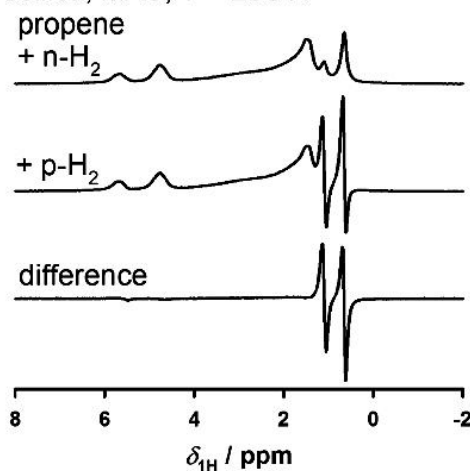


**Fig. 2**

Furthermore, the occurrence of the antiphase signals is an experimental evidence for the pairwise incorporation of  $p\text{-H}_2$  in propene molecules on platinum-loaded catalysts, as described by the mechanism in **Fig. 3** [11].

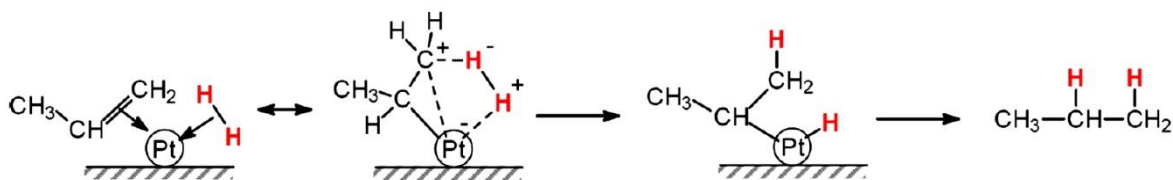


**Fig. 3**

For the separation of inphase signals of thermally polarized  $^1\text{H}$  nuclei and antiphase signals of hyperpolarized  $^1\text{H}$  nuclei, a two-dimensional (2D) nutation experiment can be utilized [12]. This approach is based on the specific properties of

hyperpolarized nuclei giving maximum signal intensities after excitation with a  $\pi/4$  pulse in contrast to thermally polarized nuclei requiring excitation by a  $\pi/2$  pulse for reaching maximum signal intensities [13, 14]. Correspondingly, during the nutation of hyperpolarized  $^1\text{H}$  nuclei in the radio frequency ( $\nu_{\text{rf}}$ ) field of a stepwise extended excitation pulse, their maximum signal intensities occur at another frequency than that of thermally polarized  $^1\text{H}$  nuclei. A similar effect is known for quadrupolar nuclei, such as  $^{23}\text{Na}$  nuclei with the spin of  $I = 3/2$  [15-17].

In **Fig. 4**, the *in situ* 2D  $^1\text{H}$  nutation MAS NMR spectrum recorded during the hydrogenation of propene with p- $\text{H}_2$  on the 0.9Pt/silica catalyst under continuous flow conditions at  $T = 373\text{ K}$  is shown [12]. The slice at  $1\ \nu_{\text{rf}}$  (top) corresponds to the spectrum consisting of the inphase signals due to thermally polarized  $^1\text{H}$  nuclei. In contrast, the slice of the nutation spectrum at  $n\ \nu_{\text{rf}}$  (bottom) shows the pure antiphase signals of hyperpolarized  $^1\text{H}$  nuclei at  $\delta_{\text{H}} = 0.6 \pm 0.2\text{ ppm}$  and  $1.0 \pm 0.2\text{ ppm}$ , caused by a pairwise incorporation of p- $\text{H}_2$  into propene molecules on the 0.9Pt/silica catalyst.

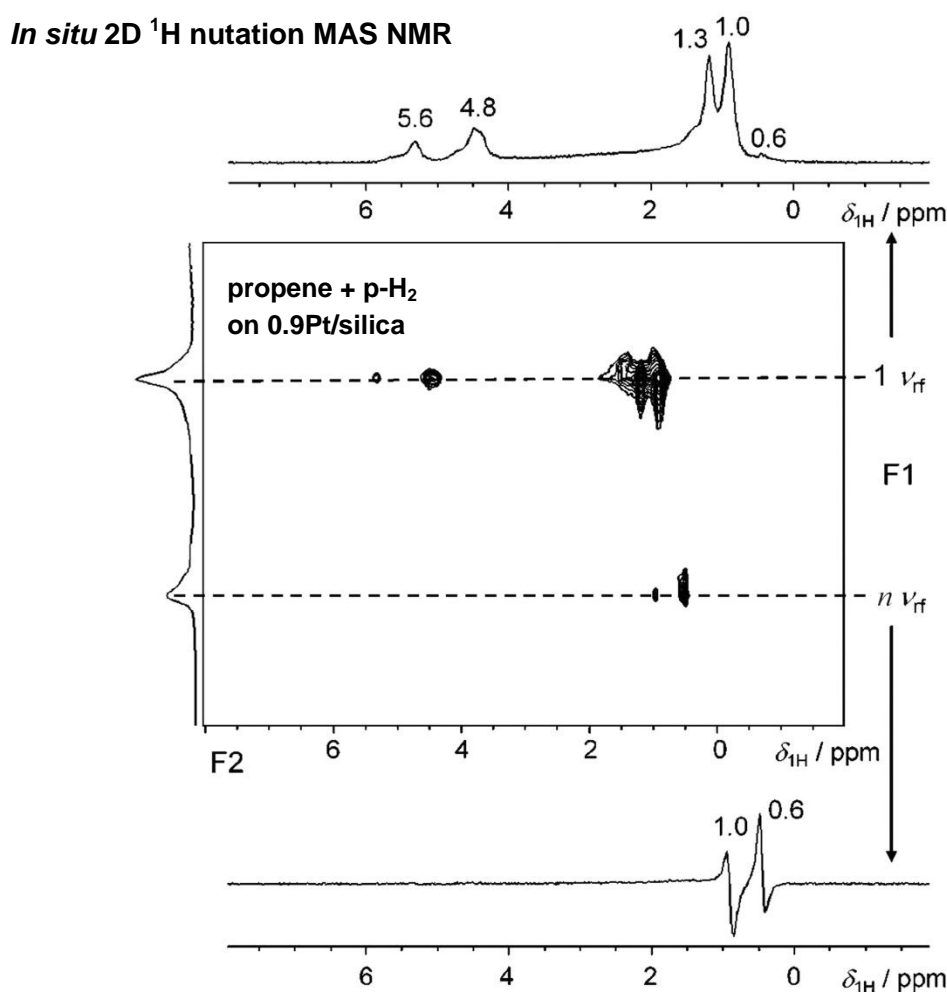


**Fig. 4**

In further experiments, the effect of the catalyst pore size and aluminum content on the intensities of the antiphase  $^1\text{H}$  NMR signals, caused by hydrogenation of propene with  $p\text{-H}_2$ , was studied (**Fig. 5**) [9]. Therefore, quantitative *in situ*  $^1\text{H}$  continuous flow MAS NMR studies of the antiphase signals, occurring during the hydrogenation of propene with  $p\text{-H}_2$  on noble metal-loaded solid catalysts with different pore sizes and different aluminium contents, were performed. For this purpose, a homologous series of samples consisting of Pt-loaded (0.9 wt.-%) silica, mesoporous SBA-15, dealuminated zeolite DeA-Y, and zeolite H,Na-Y were investigated [9]. The *in situ*  $^1\text{H}$  MAS NMR difference spectra recorded during the hydrogenation of propene with  $p\text{-H}_2$  on these catalysts are shown in **Figs. 5a to 5d, left**. All antiphase signals in these spectra have same signal shapes and positions, but different intensities. At the **right-hand side of Fig. 5**, the relative intensities of the antiphase signals are plotted as a function of the pore diameters (column 7 of Table 1 in Ref. [9]). This plot of the antiphase signal intensities hints at a dependency on the type of the siliceous support materials, i.e., silica, SBA-15, and zeolite DeA-Y. Hydrogenation of propene with  $p\text{-H}_2$  on noble metal-loaded catalysts with larger pores, such as silica, leads to larger antiphase signals than on noble metal-loaded catalysts with smaller pores, such as zeolites Y. This is a clear evidence for an enhanced relaxation of the hyperpolarized propane molecules inside small pores and *vice versa*.

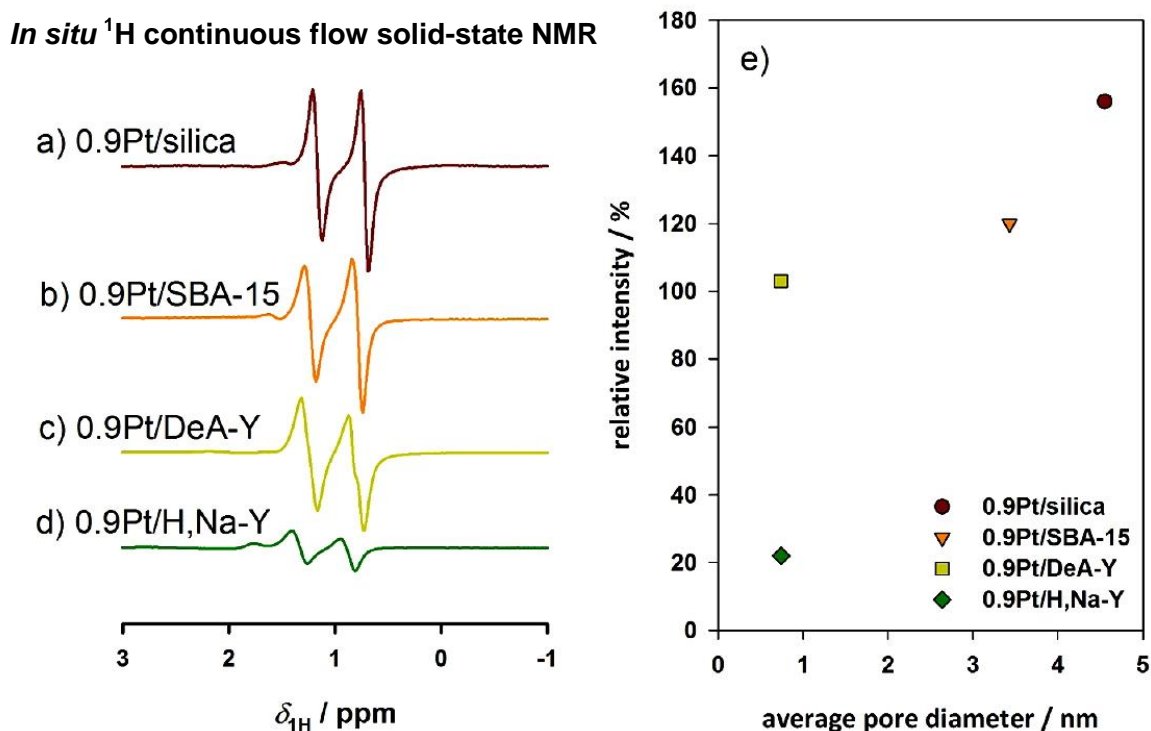


**Fig. 5**

For clarifying the effect of the amount of noble metal atoms on the experimental results, the platinum loading on silica was varied between 0.2 and 0.9 wt.-% (0.2Pt/silica, 0.5Pt/silica, and 0.9Pt/silica). *In situ*  $^1\text{H}$  MAS NMR spectroscopy during the hydrogenation of propene with  $p\text{-H}_2$  led to a less significant change of the intensity of the antiphase signals (**Table 1, lines 2 to 4, left [9]**) than observed upon variation of the type of support materials, such as observed for 0.9Pt/silica, 0.9Pt/SBA-15, and 0.9Pt/DeA-Y (see **Table 1, lines 4 to 6, left [9]**). Hence, the amount of the noble metal loading is the less critical parameter for optimizing the intensities of the antiphase signals in comparison with the morphology of different support materials.

catalyst	rel int <sup>a</sup> (%)	catalyst	rel int <sup>a</sup> (%)
0.2Pt/silica	129	0.3Rh/silica	134
0.5Pt/silica	151	0.3Rh/SBA-15	105
0.9Pt/silica	156	0.4Rh/DeA-Y	82
0.9Pt/SBA-15	120	0.4Rh/H <sub>2</sub> Na-Y	37
0.9Pt/DeA-Y	103	0.8Ir/H <sub>2</sub> Na-Y	7
0.9Pt/H <sub>2</sub> Na-Y	22	0.4Pd/H <sub>2</sub> Na-Y	4

<sup>a</sup>Determined by  $^1\text{H}$  MAS NMR spectroscopy with an accuracy of  $\pm 5\%$  using the total intensity of the spectra obtained by hydrogenation of propene with normal hydrogen ( $n\text{-H}_2$ ).

**Table 1**

Furthermore, the values summarized in **Table 1** hint at the significantly smaller antiphase signals of hyperpolarized propane formed on noble metal-loaded zeolite H<sub>2</sub>Na-Y ( $n_{\text{Si}}/n_{\text{Al}} = 2.7$ ) in comparison with zeolite DeA-Y ( $n_{\text{Si}}/n_{\text{Al}} = 93$ ) (**Table 1, lines 6 and 7, left, and lines 4 and 5, right [9]**). Hence, for support materials with same pore diameter and same noble metal loading, an enhanced relaxation of the hyperpolarized reaction products by spin interactions with framework aluminum species (spin  $I = 5/2$ ) and/or extra-framework sodium cations (spin  $I = 3/2$ ) occurs. Therefore, the focus of future *in situ* flow MAS NMR investigations of the PHIP formation on noble metal-loaded solid catalysts should be on support materials with large pores and low concentrations of relaxation sites.

Consequently, Rh-containing solicalite-1 zeolites with different particle sizes were utilized for a recent study of PHIP formation via hydrogenation of propene, comparing the ALTADENA and PASADENA protocols and applying the flow MAS NMR

technique [18]. This work supports the general findings of Ref. [9]. For a review on utilizing PHIP methods for understanding heterogeneous hydrogenation reactions, see Ref. [23].

An alternative way for utilizing hyperpolarization (HP) in NMR studies of mesoporous and microporous solids is the optical-pumping of  $^{129}\text{Xe}$  spins [19-22]. Theoretically, the optically enhanced  $^{129}\text{Xe}$  polarization can be up to 6 orders of magnitude higher than the thermal  $^{129}\text{Xe}$  polarization. Applications of HP  $^{129}\text{Xe}$  solid-state NMR spectroscopy allow obtaining information on the pore systems of solids and the diffusibility of  $^{129}\text{Xe}$  or co-adsorbed molecules. See Ref. [22] for a review on the recent state of this NMR technique.

**Catalyst preparation:** The noble metal-loaded catalysts were prepared as described in Refs. [9] and [10]. Upon the preparation, they were calcined in synthetic air (750 mL/min) by heating with a rate of 2 K/min up to  $T = 573$  K, at this temperature for 3 h, and sealed gas-tight bottles. Before the hydrogenation experiments, these samples were dehydrated and reduced in flowing hydrogen (100 mL/min) at  $T = 623$  K for 2 h, transferred into a “sample tube system 1” inside a mini glove box (see Sections “sample tube system 1” and “mini glove box”, accessible via link “*In Situ* Solid-State NMR Techniques”), purged with dry nitrogen gas, and subsequently evacuated ( $p < 10^{-2}$  Pa) at  $T = 298$  K for 12 h. The final transfer of the sample material into the 4 mm MAS rotors was performed without air contact in a mini glove box, purged with dry nitrogen gas (*vide supra*). For further details, see Refs. [9] and [10].

**In situ solid-state NMR studies:** The *in situ*  $^1\text{H}$  flow MAS NMR spectra in Figs. 2, 4, and 5 were recorded using the equipment described in the Section “equipment 3” and a 4 mm Bruker MAS NMR probe, modified as described in Section “flow probe 2”, both accessible via link “*In Situ* Solid-State NMR Techniques”,

The 4 mm Bruker MAS NMR rotors were utilized with DELRIN caps with a hole of 1.2 mm in the center. To inject hydrogen gas or the reactant mixture into the spinning 4 mm MAS NMR rotor, a glass tube with an outer diameter of 1 mm was inserted into the sample volume of the MAS rotor via the 1.2 mm hole in the rotor cap. A gap between the injection tube and the catalyst inside the MAS rotor, shaped to a hollow cylinder, ensured that no mechanical contact between this tube and the rotating catalyst can occur. Prior to the *in situ*  $^1\text{H}$  MAS NMR investigations of the propene

hydrogenation,  $40 \pm 5$  mg of dehydrated and reduced catalyst was loosely filled into a 4 mm Bruker MAS NMR rotor inside a glove box purged with dry nitrogen gas. By spinning this powder with  $\nu_{\text{rot}} = 8$  kHz for 10 min, it was pressed to a cylindrical catalyst bed allowing the insertion of the tube for the injection of the reactant mixture. The *in situ*  $^1\text{H}$  MAS NMR spectra were recorded at a Bruker Avance III 400WB spectrometer with a  $^1\text{H}$  resonance frequency of  $\nu_0 = 400.13$ , upon  $\pi/4$  single-pulse excitation, with 512 scans per spectrum, a repetition time of 0.1 s, at a spinning rate of  $\nu_{\text{rot}} \cong 4$  kHz, and with propene and p- $\text{H}_2$  flow rates of 40 and 30 mL/min, respectively, at  $T = 373$  K.

### References:

- [1] C.R. Bowers, D.P. Weitekamp, *Transformation of symmetrization order to nuclear-spin magnetization by chemical reaction and nuclear magnetic resonance*, Phys. Rev. Lett. 57 (1986) 2645-2648, DOI: [10.1103/PhysRevLett.57.2645](https://doi.org/10.1103/PhysRevLett.57.2645).
- [2] C.R. Bowers, D.P. Weitekamp, *Parahydrogen and synthesis allow dramatically enhanced nuclear alignment*, J. Am. Chem. Soc. 109 (1987) 5541-5542, DOI: [10.1021/ja00252a049](https://doi.org/10.1021/ja00252a049).
- [3] J. Natterer, J. Bargon, *Parahydrogen induced polarization*, Prog. Nucl. Magn. Reson. Spectrosc. 31 (1997) 293-315, DOI: [10.1016/S0079-6565\(97\)00007-1](https://doi.org/10.1016/S0079-6565(97)00007-1).
- [4] I.V. Skovpin, V.V. Zhivonitko, I.V. Koptug, *Parahydrogen-induced polarization in heterogeneous hydrogenations over silica-immobilized Rh complexes*, Appl. Magn. Reson. 41 (2011) 393-410, DOI: [10.1007/s00723-011-0255-z](https://doi.org/10.1007/s00723-011-0255-z).
- [5] S.B. Duckett, N.J. Wood, *Parahydrogen-based NMR methods as a mechanistic probe in inorganic chemistry*, Coord. Chem. Rev. 252 (2008) 2278-2291, DOI: [10.1016/j.ccr.2008.01.028](https://doi.org/10.1016/j.ccr.2008.01.028).
- [6] I.V. Koptug, V.V. Zhivonitko, K.V. Kovtunov, *New perspectives for parahydrogen-induced polarization in liquid phase heterogeneous hydrogenation: An aqueous phase and ALTADENA study*, ChemPhysChem 11 (2010) 3086-3088, DOI: [10.1002/cphc.201000407](https://doi.org/10.1002/cphc.201000407).
- [7] D. Canet, S. Bouguet-Bonnet, C. Aroulanda, F. Reinert, *About long-lived nuclear spin states involved in para-hydrogenated molecules*, J. Am. Chem. Soc. 129 (2007) 1445-1449, DOI: [10.1021/ja066313x](https://doi.org/10.1021/ja066313x).
- [8] P.J. Carson, C.R. Bowers, D.P. Weitekamp, *The PASADENA effect at a solid surface: High-sensitivity nuclear magnetic resonance of hydrogen chemisorption*, J. Am. Chem. Soc. 123 (2001) 11821-11822, DOI: [10.1021/ja010572z](https://doi.org/10.1021/ja010572z).



- [9] U. Obenaus, S. Lang, R. Himmelmann, M. Hunger, *In situ MAS NMR investigation of parahydrogen induced hyperpolarization inside meso- and micropores of Ir-, Pt-, Rh-, and Pd-containing solid catalysts*, J. Phys. Chem. C 121 (2017) 9953-9962, DOI: [10.1021/acs.jpcc.7b01899](https://doi.org/10.1021/acs.jpcc.7b01899).
- [10] H. Henning, M. Dyballa, M. Scheibe, E. Klemm, M. Hunger, *In situ CF MAS NMR study of the pairwise incorporation of parahydrogen into Olefins on rhodium-containing zeolites Y*, Chem. Phys. Lett. 555 (2013) 258-262, DOI: [10.1016/j.cplett.2012.10.068](https://doi.org/10.1016/j.cplett.2012.10.068).
- [11] S.S. Arzumanov, A.G. Stepanov, *Parahydrogen-induced polarization detected with continuous flow magic angle spinning NMR*, J. Phys. Chem. C 117 (2013) 2888–2892, DOI: [10.1021/jp311345r](https://doi.org/10.1021/jp311345r).
- [12] U. Obenaus, G. Althoff-Ospelt, S. Lang, R. Himmelmann, M. Hunger, *Separation of anti-phase signals due to para-hydrogen induced polarization via 2D nutation NMR spectroscopy*, ChemPhysChem 18 (2017) 455-458, DOI: [10.1002/cphc.201601227](https://doi.org/10.1002/cphc.201601227).
- [13] D. Canet, *Nuclear Magnetic Resonance: Concepts and Methods*, 1st ed., John Wiley & Sons, New York, 1996, ISBN-13: [978-0471961451](https://doi.org/978-0471961451).
- [14] D. Canet, C. Aroulanda, P. Mutzenhardt, S. Aime, R. Gobetto, F. Reineri, *Para-hydrogen enrichment and hyperpolarization*, Concepts in Magnetic Resonance A 28 (2006) 321-330, DOI: [10.1002/cmr.a.20065](https://doi.org/10.1002/cmr.a.20065).
- [15] D. Fenzke, D. Freude, T. Froehlich, J. Haase, *NMR intensity measurements of half-integer quadrupole nuclei*, Chem. Phys. Lett. 111 (1984) 171-175, DOI: [10.1016/0009-2614\(84\)80458-3](https://doi.org/10.1016/0009-2614(84)80458-3).
- [16] A. P. M. Kentgens, J. J. M. Lemmens, F. M. M. Guerts, W. S. Veeman, *Two-dimensional solid-state nutation NMR of half-integer quadrupolar nuclei*, J. Magn. Reson. 71 (1987) 62-74, DOI: [10.1016/0022-2364\(87\)90127-2](https://doi.org/10.1016/0022-2364(87)90127-2).
- [17] M. Hunger, G. Engelhardt, H. Koller, J. Weitkamp, *Characterization of sodium cations in dehydrated faujasites and zeolite EMT by  $^{23}\text{Na}$  DOR, 2D nutation, and MAS NMR*, Solid State Nucl. Magn. Reson. 2 (1993) 111-120, DOI: [10.1016/0926-2040\(93\)90029-M](https://doi.org/10.1016/0926-2040(93)90029-M).
- [18] W. Wang, J. Xu, Q. Sun, F. Deng, *Heterogeneous parahydrogen induced polarization on Rh-containing silicalite-1 zeolites: Effect of the catalyst structure on signal enhancement*, Catal. Sci. Technol. 12 (2022) 4442–4449, DOI: [10.1039/d2cy00615d](https://doi.org/10.1039/d2cy00615d).
- [19] E. Brunner, R. Seydoux, M. Haake, A. Pines, J. A. Reimer, *Surface NMR using laser-polarized  $^{129}\text{Xe}$  under magic angle spinning conditions*, J. Magn. Reson. 130 (1998) 145–148, DOI: [10.1006/jmre.1997.1296](https://doi.org/10.1006/jmre.1997.1296).

- [20] A. Nossov, F. Guenneau, M.A. Springuel-Huet, E. Haddad, V. Montouillout, B. Knott, F. Engelke, C. Fernandez, A. Gedeon, *Continuous flow hyperpolarized  $^{129}\text{Xe}$ -MAS NMR studies of microporous materials*, Phys. Chem. Chem. Phys. 5 (2003) 4479-4483, DOI: [10.1039/b305793n](https://doi.org/10.1039/b305793n).
- [21] S. T. Xu, W. P. Zhang, X. C. Liu, X. W. Han, X. H. Bao, *Enhanced in situ continuous-flow MAS NMR for reaction kinetics in the nanocages*, J. Am. Chem. Soc. 131 (2009) 13722-13727, DOI: [10.1021/ja904304h](https://doi.org/10.1021/ja904304h).
- [22] B. Fan, S. Xu, Y. Wei, Z. Liu, *Progresses of hyperpolarized  $^{129}\text{Xe}$  NMR application in porous materials and catalysis*, Magn. Reson. Lett. 1 (2021) 11-27, DOI: [10.1016/j.mrl.2021.100005](https://doi.org/10.1016/j.mrl.2021.100005).
- [23] W. Wang, Q. Wang, J. Xu, F. Deng, *Understanding heterogeneous catalytic hydrogenation by parahydrogen-induced polarization NMR spectroscopy*, ACS Catal. 13 (2023) 3501-3519, DOI: [10.1021/acscatal.2c05659](https://doi.org/10.1021/acscatal.2c05659).